Preprint number: XXXX-XXXX

Confining potential under the gauge field condensation in the SU(2) Yang-Mills theory

Hirohumi Sawayanagi†

$Q\bar{Q}$ potential is studied in the SU(2) gauge theory. Based on the nonlinear gauge of the Curci-Ferrari type, the possibility of a gluon condensation $\langle A_\mu^+ A_\mu^- \rangle$ in low-energy region has been considered at the one-loop level. Instead of the magnetic monopole condensation, this condensation makes classical gluons massive, and can yield a linear potential. We show this potential consists of the Coulomb plus linear part and an additional part. Comparing with the Cornell potential, we study this confining potential in detail, and find that the potential has two implicit scales r_c and $\tilde{R}_0$. The meanings of these scales are clarified. We also show that the Cornell potential that fits well to this confining potential is obtained by taking these scales into account.

Subject Index B0,B3,B6

arXiv:2008.03431v3 [hep-ph] 21 Jan 2021

† National Institute of Technology, Kushiro College, Kushiro, 084-0916, Japan
E-mail:sawa@kushiro-ct.ac.jp

typeset using $\mathcal{PTP}$TEX.cls

1 Introduction

In the study of quarkonia, QCD potential is often used. Although there are some phenomenological potentials (see, e.g., [1]), the Cornell potential $V_{CL}(r)$ [2, 3] is simple but workable. This potential has the Coulomb plus linear form as

$$V_{CL}(r) = -\frac{K}{r} + \sigma r, \tag{1.1}$$

where K and σ, that is called the string tension, are constants. The Coulomb part is expected from the perturbative one-gluon exchange, and the linear part represents the confinement.

Is it possible to derive $V_{CL}(r)$ from QCD? Using the dual Ginzburg-Landau model (see, e.g., [4]), the following Yukawa plus linear potential was obtained [5–8]:

$$V_{YL}(r) = -\frac{Q^2}{4\pi}\frac{e^{-mr}}{r} + \left(\frac{Q^2m^2}{8\pi}\ln\frac{m^2+m_\chi^2}{m^2}\right)r, \tag{1.2}$$

where Q is the static quark charge and m_χ is the momentum cut-off. In this model, the mass m is related to the vacuum expectation value (VEV) of the monopole field. In Ref. [9], based on the SU(2) gauge theory in the non-linear gauge of the Curci-Ferrari type, we also derived the potential $V_{YL}(r)$. In this case, the mass m comes from the gauge field condensation $\langle A_\mu^+ A_\mu^-\rangle$.

In this paper, in the framework of Refs. [9, 10], we restudy the confining potential. In the next section, we briefly review Refs. [9, 10], and present the potential between the static charges Q and $\bar{Q}$. In Sect. 3, the equation to determine an ultraviolet cut-off Λ_c is derived. In Sect. 4, using this cut-off, we show that the $Q\bar{Q}$ potential becomes the confining potential $V_c(r) = V_{CL}(r) + V_3(r)$, where $V_3(r)$ is the additional potential. The potential $V_c(r)$ has several parameters. Comparing $V_c(r)$ with $V_{CL}(r)$, and choosing the appropriate values of K and σ, the parameters in $V_c(r)$ are determined in Sect. 5. In this process, we find a scale $r_c \approx 0.2$ fm. In the intermediate region, the scale $R_0 \approx 0.5$ fm has been proposed [11]. The meanings of the scales r_c and R_0 for $V_c(r)$ are clarified in Sect. 6. We also propose a scale $\tilde{R}_0$ that is related to R_0. Based on this analysis, we obtain $V_{CL}(r)$ that fits well to $V_c(r)$. Section 7 is devoted to a summary and comments. In Appendix A, the propagator for the off-diagonal gluons is presented. The equations in Sect. 5, that determine the values of the parameters in $V_c(r)$, are solved in Appendix B.

2 Condensate $\langle A_\mu^+ A_\mu^-\rangle$ and $Q\bar{Q}$ potential

In this section, we review Refs. [9, 10] briefly.

2.1 Ghost condensation

We consider the SU(2) gauge theory in Euclidean space. The Lagrangian in the nonlinear gauge of the Curci-Ferrari type [12] is

$$\mathcal{L} = \mathcal{L}_{inv} + \mathcal{L}_{NL}, \quad \mathcal{L}_{inv} = \frac{1}{4}F_{\mu\nu}^2,$$
$$\mathcal{L}_{NL} = B \cdot \partial_\mu A_\mu + i\bar{c} \cdot \partial_\mu D_\mu c - \frac{\alpha_1}{2}B^2 - \frac{\alpha_2}{2}\bar{B}^2 - B \cdot w, \tag{2.1}$$

where B is the Nakanishi-Lautrup field, c ($\bar{c}$) is the ghost (antighost), $\bar{B} = -B + ig\bar{c} \times c$, α_1 and α_2 are gauge parameters, and w is a constant to keep the BRS symmetry. Introducing the auxiliary field φ, which represents $\alpha_2\bar{B}$, $\mathcal{L}_{NL}$ is rewritten as [13]

$$\mathcal{L}_\varphi = -\frac{\alpha_1}{2}B^2 + B \cdot (\partial_\mu A_\mu + \varphi - w) + i\bar{c} \cdot (\partial_\mu D_\mu + g\varphi\times)c + \frac{\varphi^2}{2\alpha_2}. \tag{2.2}$$

In Ref. [14], by integrating out $\bar{c}$ and c with momentum $\mu \le p \le \Lambda$, we studied the one-loop effective potential for φ, and showed that $g\varphi^A$ acquires the VEV $g\varphi_0\delta^{A3}$ under an energy scale μ_0. The scale μ_0 and the VEV $v = g\varphi_0$ are

$$\mu_0 = \Lambda e^{-4\pi^2/(\alpha_2 g^2)}, \; v = \left\{ \frac{\mu_0^4 - \mu^4}{1 - e^{-16\pi^2/(\alpha_2 g^2)}} \right\}^{1/2}. \tag{2.3}$$

At the one-loop order, it is shown that $\alpha_2 = \beta_0/2$ is the ultraviolet fixed point, where $\beta_0 = 22/3$ is the first coefficient of the renormalization group function β for SU(2). So, when $\Lambda \gg \mu_0 \gg \mu$, the relation

$$\mu_0 = \Lambda_{\rm QCD}, \quad v \simeq \Lambda_{\rm QCD}^2 \tag{2.4}$$

holds [14], where $\Lambda_{\rm QCD}$ is the QCD scale parameter.

2.2 Condensate $\langle A_\mu^+ A_\mu^- \rangle$

When $v \neq 0$, the ghost Lagrangian becomes

$$i\sum_{a=1}^{2}\left(\bar{c}^a\Box c^a - \sum_{b=1}^{2} v\epsilon_{ab}\bar{c}^a c^b\right) + i\bar{c}^3\Box c^3. \tag{2.5}$$

Because of the v term in Eq.(2.5), the two-point function

$$\langle A_\mu^+(y) A_\nu^-(x)\rangle = G_{\mu\nu}(y,x)$$

shows the tachyonic behavior. In fact, the ghost loop depicted in Fig. 1(b) yields the tachyonic mass $(-g^2 v)/(64\pi)$ for A_μ^a $(a = 1, 2)$ in the low momentum limit $p \to 0$. In the same way, A_μ^3 has the tachyonic mass $-g^2 v/(32\pi)$ in this limit.

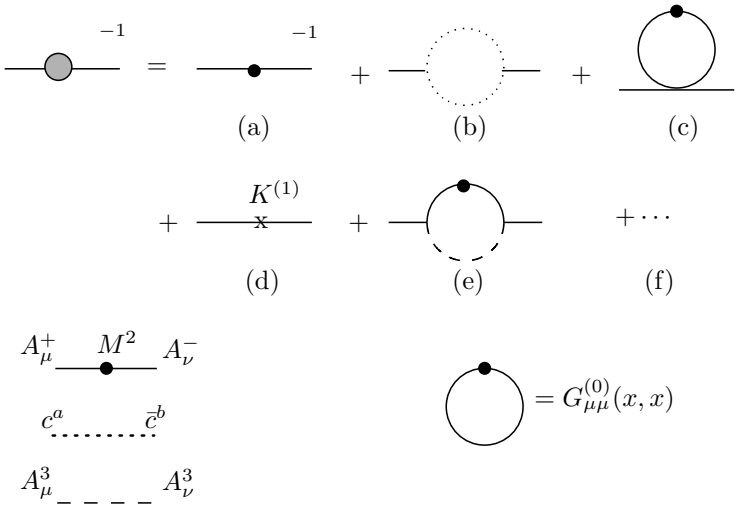


Fig. 1 The diagrams that contribute to the inverse propagator for $A^\pm_\mu$. Fig. 1(b) yields the tachyonic mass in the limit $p \to 0$, and Fig. 1(c) brings about the VEV $G^{(0)}_{\mu\mu}(x,x)$.

To remove the tachyonic mass terms

$$\frac{1}{2}\left(\frac{-g^2 v}{64\pi}\right)\left\{\sum_{a=1}^{2}(A^a_\mu)^2 + 2(A^3_\mu)^2\right\}, \tag{2.6}$$

we introduce the source term

$$K A^+_\mu A^-_\mu, \quad K = K^{(0)} + K^{(1)} + \cdots, \quad K^{(n)} = O(\hbar^n).$$

Although the source K may depend on the momentum scale, for simplicity, we treat it as constant, and write $K^{(0)} = M^2$. To consider the inverse propagator for $A^\pm_\mu$ depicted in Fig. 1 in the limit $p \to 0$, we write the free part of the propagator $G_{\mu\nu}(y,x)$ as $G^{(0)}_{\mu\nu}(y,x)$. Then the diagram in Fig. 1(c) gives the VEV $g^2 G^{(0)}_{\mu\mu}(x,x)$. If $K^{(1)}$ subtracts divergent terms of $O(\hbar)$ in this limit, the condition

$$G^{(0)}_{\mu\mu}(x,x) = \frac{v}{64\pi}, \tag{2.7}$$

removes the tachyonic mass for $A^\pm_\mu$. Because of the interaction $g^2(A^+_\mu A^-_\mu)(A^3_\nu)^2$ in $F^2_{\mu\nu}/4$, this VEV also removes the tachyonic mass for A^3_μ.

2.3 Inclusion of a classical solution

To introduce a classical solution, the gauge field A^A_μ is divided into the classical part $b^A_\mu = b_\mu \delta^{A3}$ and the quantum part a^A_μ, i.e., $A^\pm_\mu = a^\pm_\mu,\ A^3_\mu = b_\mu + a^3_\mu$. As the tachyonic masses

come from the ghost loops with the VEV v, it is expected that b_μ acquires no tachyonic mass. To see it, we divide the gauge transformation $\delta A_\mu = D_\mu(A)\varepsilon$ as

$$\delta a_\mu = D_\mu(a)\varepsilon, \quad \delta b_\mu = g b_\mu \times \varepsilon,$$

where $D_\mu(A) = (\partial_\mu + g A_\mu \times)$. Then, using the gauge-fixing function $G = \partial_\mu a_\mu + \varphi - w$, the ghost Lagrangian

$$B \cdot [\partial_\mu a_\mu + \varphi - w] + i\bar{c} \cdot [\partial_\mu D_\mu(a) + g\varphi \times] c$$

is obtained. If A_μ is replaced by a_μ, Eq.(2.2) becomes this Lagrangian. So, the tachyonic mass terms for a_μ^A are

$$\frac{1}{2}\left(\frac{-g^2 v}{64\pi}\right)\left\{\sum_{a=1}^{2}(a_\mu^a)^2 + 2(a_\mu^3)^2\right\},$$

and b_μ acquires no tachyonic mass. [1]

Next, we consider the effect of the VEV $G^{(0)}_{\mu\mu}(x,x)$. As in the previous subsection, these tachyonic mass terms for a_μ^A are removed by the VEV in Eq.(2.7). In addition, the interaction $g^2(A_\mu^+ A_\mu^-)(a_\nu^3 + b_\nu)^2$ in $F_{\mu\nu}^2/4$ generates the mass term

$$\frac{m^2}{2}(b_\nu)^2, \quad m^2 = 2g^2 G^{(0)}_{\mu\mu}(x,x). \tag{2.8}$$

Thus, after integrating out c and $\bar{c}$, an effective low energy Lagrangian becomes

$$\begin{aligned}\mathcal{L} =& \frac{1}{4}(\partial \wedge b)_{\mu\nu}(\partial \wedge b)_{\mu\nu} + \frac{m^2}{2} b_\mu b_\mu + \frac{1}{4}(\partial \wedge a^3)_{\mu\nu}(\partial \wedge a^3)_{\mu\nu} \\ &+ \frac{1}{2}(\partial \wedge A^+)_{\mu\nu}(\partial \wedge A^-)_{\mu\nu} + M^2 A_\mu^+ A_\mu^- + \cdots,\end{aligned} \tag{2.9}$$

where $(\partial \wedge A)_{\mu\nu} = \partial_\mu A_\nu - \partial_\nu A_\mu$. Namely, although the quantum part a_μ^3 is massless, the classical part b_μ has the mass m. The off-diagonal components $A_\mu^\pm$ have the mass M determined by the equation

$$\frac{v}{64\pi} = G^{(0)}_{\mu\mu}(x,x). \tag{2.10}$$

2.4 $Q\bar{Q}$ potential

Now we consider the confining potential. As the classical field b_μ, we choose the dual electric potential $\mathcal{B}_\mu$, that describes the electric monopole solution [9]. The color electric

[1] In Ref. [10], using the background covariant gauge-fixing, we showed, although the ghost Lagrangian contains b_μ, it does not acquire the tachyonic mass.

current j_μ is incorporated by the replacement

$$(\partial \wedge \mathcal{B})_{\mu\nu} \to (\partial \wedge \mathcal{B})_{\mu\nu} + \epsilon_{\mu\nu\alpha\beta}(n\cdot\partial)^{-1} n_\alpha j_\beta,$$

where the space-like vector n_μ [15] is chosen as $n_\mu = (0, \boldsymbol{n})$ with $\boldsymbol{n}\cdot\boldsymbol{n} = 1$, and $n\cdot\partial = n_\mu\partial_\mu$. We note this is the Zwanziger's dual field strength $F^d = (\partial \wedge B) + (n\cdot\partial)^{-1}(n \wedge j_e)^d$ in Ref. [15]. Thus the classical part of $\mathcal{L}$ in Eq.(2.9) becomes

$$\frac{1}{4}\left[(\partial \wedge \mathcal{B})_{\mu\nu} + \epsilon_{\mu\nu\alpha\beta}(n\cdot\partial)^{-1} n_\alpha j_\beta\right]^2 + \frac{m^2}{2}\mathcal{B}_\mu\mathcal{B}_\mu. \tag{2.11}$$

The equation of motion for $\mathcal{B}_\mu$ is

$$(D_m^{-1})_{\mu\nu}\mathcal{B}_\nu = \epsilon_{\mu\rho\alpha\beta}(n\cdot\partial)^{-1} n_\rho\partial_\alpha j_\beta, \quad (D_m^{-1})_{\mu\nu} = (-\Box + m^2)\delta_{\mu\nu} + \partial_\mu\partial_\nu,$$

and $\mathcal{B}_\mu$ is solved as

$$\mathcal{B}_\mu = (D_m)_{\mu\nu}\epsilon_{\nu\rho\alpha\beta}(n\cdot\partial)^{-1} n_\rho\partial_\alpha j_\beta, \quad (D_m)_{\mu\nu} = \frac{\delta_{\mu\nu} - \partial_\mu\partial_\nu/\Box}{-\Box + m^2} + \frac{\partial_\mu\partial_\nu}{m^2\Box}. \tag{2.12}$$

If we use Eq.(2.12), Eq.(2.11) becomes

$$\mathcal{L}_{jj} = \frac{1}{2}j_\mu\frac{1}{-\Box + m^2}j_\mu - \frac{1}{2}j_\mu\frac{m^2}{-\Box + m^2}\frac{n\cdot n}{(n\cdot\partial)^2}\left(\delta_{\mu\nu} - \frac{n_\mu n_\nu}{n\cdot n}\right)j_\nu. \tag{2.13}$$

To derive the static potential between the color electric charges Q and $-Q$, the static current

$$j_\mu(x) = Q\delta_{\mu 0}\{\delta(\boldsymbol{x} - \boldsymbol{a}) - \delta(\boldsymbol{x} - \boldsymbol{b})\} \tag{2.14}$$

is substituted into $\mathcal{L}_{jj}$. Then it leads to the potential

$$\begin{aligned} V(r) =& V_Y(r) + V_L(r), \quad V_Y = Q^2\int\frac{d^3q}{(2\pi)^3}\frac{1-\cos\boldsymbol{q}\cdot\boldsymbol{r}}{q^2+m^2}, \\ & V_L = Q^2\int\frac{d^3q}{(2\pi)^3}(1-\cos\boldsymbol{q}\cdot\boldsymbol{r})\frac{m^2}{(q^2+m^2)q_n^2}, \end{aligned} \tag{2.15}$$

where $\boldsymbol{r} = \boldsymbol{a} - \boldsymbol{b}$, $q = |\boldsymbol{q}|$ and $q_n = \boldsymbol{q}\cdot\boldsymbol{n}$. Although the term V_Y (V_L) becomes the Yukawa (linear) potential in Eq.(1.2) usually, we restudy Eq.(2.15) in Sect. 4.

3 Cut-off Λ_c and the mass M

In this section, we study Eq.(2.10). The free propagator $G^{(0)}_{\mu\nu}(p)$ is calculated in Appendix A as

$$G^{(0)}_{\mu\nu}(p) = \frac{1}{p^2+M^2}P^T_{\mu\nu} + \frac{1}{M^2}P^L_{\mu\nu}, \quad P^T_{\mu\nu} = \delta_{\mu\nu} - \frac{p_\mu p_\nu}{p^2}, \quad P^L_{\mu\nu} = \frac{p_\mu p_\nu}{p^2}. \tag{3.1}$$

Assuming that M exists below a cut-off Λ_c, we obtain

$$G^{(0)}_{\mu\mu}(x,x) = \int_0^{\Lambda_c}\frac{d^4p}{(2\pi)^4}G^{(0)}_{\mu\mu}(p) = \frac{1}{(4\pi)^2}\left\{\frac{\Lambda_c^4}{2M^2} - 3M^2\ln\left(1+\frac{\Lambda_c^2}{M^2}\right)\right\}, \tag{3.2}$$

where the M-independent term Λ_c^2 is subtracted.

The VEV v depends on the momentum scale μ. From Eqs.(2.3) and (2.4), we find v disappears above the scale $\mu_0 = \Lambda_{\rm QCD}$. When $0 \leq \mu \leq \Lambda_{\rm QCD}$, v behaves as

$$v \to 0 \quad (\mu \to \Lambda_{\rm QCD}), \quad v \to \Lambda_{\rm QCD}^2 \quad (\mu \to 0).$$

Namely the maximal value of v is $\Lambda_{\rm QCD}^2$, and the left hand side of Eq.(2.10) satisfies

$$0 \leq \frac{v}{64\pi} \leq \frac{\Lambda_{\rm QCD}^2}{64\pi}.$$

On the other hand, the VEV $G^{(0)}_{\mu\mu}(x,x)$ only depends on the constants M and Λ_c. Since the tachyonic mass should be removed in the overall momentum region completely, using the maximal value of v, we interpret Eq.(2.10) as [2]

$$\frac{\Lambda_{\rm QCD}^2}{64\pi} \simeq G^{(0)}_{\mu\mu}(x,x). \tag{3.3}$$

From Eqs.(3.2) and (3.3), we obtain

$$\frac{\pi}{2}\frac{\Lambda_{\rm QCD}^2}{M^2} \simeq \frac{\Lambda_c^4}{M^4} - 6\ln\left(1 + \frac{\Lambda_c^2}{M^2}\right). \tag{3.4}$$

We make a comment. Eq.(3.4) determines the relation of M and Λ_c so as to give the maximal value of v. Using Eq.(3.3), we find $m^2 = 2g^2 G^{(0)}_{\mu\mu}(x,x) \simeq g^2\Lambda_{\rm QCD}^2/(32\pi)$. Although the VEV v depends on the scale μ, and disappears above $\Lambda_{\rm QCD}$, $G^{(0)}_{\mu\mu}(x,x)$ does not. So the mass m can survive above the scale $\Lambda_{\rm QCD}$.

4 Confining potential

Usually, the potential V in Eq.(2.15) is calculated as follows. Let us divide the momentum $\boldsymbol{q}$ in V_L into $q_n = \boldsymbol{q}\cdot\boldsymbol{n}$ and $\boldsymbol{q}_T$ that satisfies $\boldsymbol{q}_T \cdot \boldsymbol{n} = 0$. Then the integral of q_n has the infrared divergence, and the integral of $q_T = |\boldsymbol{q}_T|$ has the ultraviolet divergence. The former divergence is removed by the choice $\boldsymbol{r} \parallel \boldsymbol{n}$ [7, 9], and the latter divergence is avoided by the

[2] If we consider the scale dependent M, Eq.(3.2) should be replaced by the integral

$$\int_0^{\Lambda_c} \frac{d^4p}{(2\pi)^4}\left\{\frac{P^T_{\mu\nu}}{p^2 + M(p)^2} + \frac{P^L_{\mu\nu}}{M(p)^2}\right\}.$$

As $M(p)$ is unknown, we cannot calculate it. But it is also μ-independent.

cut-off m_χ as [5–8]

$$V_L = \frac{Q^2 m^2}{(2\pi)^2}\int_{-\infty}^{\infty} dq_n \int_0^{m_\chi} dq_T q_T \frac{1-\cos q_n r}{(q_n^2+q_T^2+m^2)q_n^2}. \tag{4.1}$$

Eq.(4.1) becomes the linear term in Eq.(1.2). The term V_Y has the integral of $q=|\boldsymbol{q}|$ over the region of $0 \le q < \infty$, and the Yukawa potential in Eq.(1.2) is obtained.

To introduce a cut-off in a different way, we write the potential as

$$V(r) = \int dq W(\boldsymbol{q}, m, r). \tag{4.2}$$

As we stated in Sect. 3, the mass m can exist above $\Lambda_{\rm QCD}$. From Fig. 1(c), after v disappears, it is expected that m^2 contributes to the correction for M^2. Since $A_\mu^\pm$ are considered to be massless above Λ_c, we assume that the cut-off for m is Λ_c, and define Eq.(4.2) as

$$V(r) = \int_0^{\Lambda_c} dq W(\boldsymbol{q}, m, r) + \int_{\Lambda_c}^{\infty} dq W(\boldsymbol{q}, 0, r). \tag{4.3}$$

Eq.(4.3) is rewritten as

$$V(r) = \int_0^{\infty} dq W(\boldsymbol{q}, 0, r) + \int_0^{\Lambda_c} dq \left\{W(\boldsymbol{q}, m, r) - W(\boldsymbol{q}, 0, r)\right\}. \tag{4.4}$$

The first term becomes

$$\int_0^{\infty} dq W(\boldsymbol{q}, 0, r) = V_1(r) = Q^2 \int_{D_\infty} \frac{d^3q}{(2\pi)^3}\frac{1-\cos \boldsymbol{q}\cdot\boldsymbol{r}}{q^2}, \quad D_\infty = \{q \mid 0 \le q < \infty\}, \tag{4.5}$$

and the second term leads to

$$\begin{aligned}
&\int_0^{\Lambda_c} dq \left\{W(\boldsymbol{q}, m, r) - W(\boldsymbol{q}, 0, r)\right\} = V_2(r) + V_3(r), \\
&V_2(r) = Q^2 \int_{D_{\Lambda_c}} \frac{d^3q}{(2\pi)^3}(1-\cos \boldsymbol{q}\cdot\boldsymbol{r})\frac{m^2}{(q^2+m^2)q_n^2}, \\
&V_3(r) = -Q^2 \int_{D_{\Lambda_c}} \frac{d^3q}{(2\pi)^3}(1-\cos \boldsymbol{q}\cdot\boldsymbol{r})\frac{m^2}{(q^2+m^2)q^2}, \quad D_{\Lambda_c} = \{q \mid 0 \le q < \Lambda_c\},
\end{aligned} \tag{4.6}$$

where $V_2(r)$ ($V_3(r)$) comes from V_L ($V_Y(m^2) - V_Y(m^2=0)$). Eq.(4.5) gives the usual Coulomb potential

$$V_1(r) = -\frac{K_c}{r}, \quad K_c = \frac{Q^2}{4\pi}. \tag{4.7}$$

Now we consider $V_2(r)$. To satisfy $0 \le q \le \Lambda_c$, the domain of integration is not ($-\infty < q_n < \infty, 0 \le q_T \le m_\chi$) in Eq.(4.1), but ($-\varepsilon \le q_n \le \varepsilon, 0 \le q_T \le \sqrt{\Lambda_c^2 - \varepsilon^2}$) with $0 < \varepsilon \ll 1$,

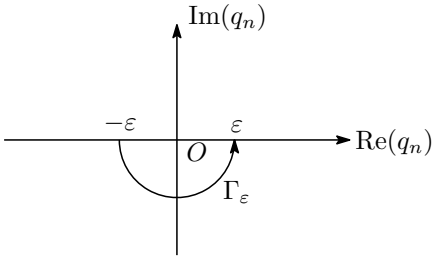


Fig. 2 The integration path Γ_ε for q_n.

i.e.,

$$V_2(r) = \frac{Q^2m^2}{(2\pi)^2}\int_0^{\sqrt{\Lambda_c^2-\varepsilon^2}} dq_T q_T \int_{-\varepsilon}^{\varepsilon} dq_n \frac{1-e^{iq_nr}}{q_n^2(q_n^2+q_T^2+m^2)}.$$

Since the integrand is singular at $q_n = 0$, we choose the anticlockwise path Γ_ε in Fig. 2, and take the limit $\varepsilon \to 0$. Then we obtain

$$V_2(r) = \frac{Q^2m^2}{(2\pi)^2}\int_0^{\Lambda_c} dq_T q_T \frac{\pi r}{q_T^2+m^2} = \sigma_c r, \quad \sigma_c = \frac{Q^2m^2}{8\pi}\ln\left(\frac{\Lambda_c^2+m^2}{m^2}\right). \tag{4.8}$$

If the cut-off Λ_c is replaced by m_χ, $V_2(r)$ becomes the linear term in Eq.(1.2).

Finally, neglecting additive constants, we find $V_3(r)$ becomes

$$V_3(r) = \frac{Q^2m^2}{2\pi^2}\int_0^{\Lambda_c} dq \frac{\sin qr}{qr}\frac{1}{q^2+m^2}. \tag{4.9}$$

Thus the confining potential we propose is

$$V_c(r) = \sum_{k=1}^{3} V_k(r) = -\frac{K_c}{r} + \sigma_c r + \frac{Q^2m^2}{2\pi^2}\int_0^{\Lambda_c} dq \frac{\sin qr}{qr}\frac{1}{q^2+m^2}. \tag{4.10}$$

In addition to the Coulomb plus linear part, there is the term $V_3(r)$.

5 Determination of parameters

Although we presented the potential $V_c(r) = \sum_{k=1}^{3} V_k(r)$, the values of the parameters Q^2 and m are unknown. To determine them, let us expand a potential $V(r)$ as

$$V(r) = V(r_c) + V'(r_c)(r-r_c) + \frac{V''(r_c)}{2}(r-r_c)^2 + \frac{V^{(3)}(r_c)}{3!}(r-r_c)^3 + \cdots .$$

We assume there is a true confining potential $V_T(r)$. Then we require the Cornell potential $V_{CL}(r)$ fits well to $V_T(r)$ at a point $r = r_c$. This is achieved by choosing (K, σ) and the

constant $V(r_c)$ appropriately. [3] We impose the conditions

$$V_T^{(n)}(r_c) = V_{CL}^{(n)}(r_c), \quad (n = 0, 1, 2), \tag{5.1}$$

and determine (K, σ) and $V(r_c)$.

Next, we require that the potential $V_c(r)$ fits well to this $V_{CL}(r)$ at $r = r_c$, and use the conditions

$$V_{CL}^{(n)}(r_c) = V_c^{(n)}(r_c), \quad (n = 0, 1, 2, 3). \tag{5.2}$$

We note, to determine the parameters Q^2 and m, the two conditions with $n = 1, 2$ are necessary. However, to determine r_c, the condition with $n = 3$ is required.

From Eqs.(1.1) and (4.10), we have

$$\begin{aligned} &-\frac{r^3}{2}V_{CL}''(r) = K, \quad \frac{1}{2r}\left(r^2 V_{CL}'(r)\right)' = \sigma, \\ &-\frac{r^3}{2}V_c''(r) = K_c - \frac{r^3}{2}V_3''(r), \quad \frac{1}{2r}\left(r^2 V_c'(r)\right)' = \sigma_c + \frac{1}{2r}\left(r^2 V_3'(r)\right)'. \end{aligned}$$

Since Eq.(5.2) with $n = 2$ gives $r_c^3 V_{CL}''(r_c) = r_c^3 V_c''(r_c)$, this condition becomes

$$K = K_{ef}(r_c), \quad K_{ef}(r_c) = K_c - \frac{r_c^3}{2}V_3''(r_c). \tag{5.3}$$

In the same way, the condition $\left(r_c^2 V_{CL}'(r_c)\right)' = \left(r_c^2 V_C'(r_c)\right)'$ leads to

$$\sigma = \sigma_{ef}(r_c), \quad \sigma_{ef}(r_c) = \sigma_c + \frac{1}{2r_c}\left(r_c^2 V_3'(r_c)\right)', \tag{5.4}$$

and $\left(r_c^3 V_{CL}''(r_c)\right)' = \left(r_c^3 V_c''(r_c)\right)'$ becomes

$$\left(r_c^3 V_3''(r_c)\right)' = 0. \tag{5.5}$$

Of course, the true potential $V_T(r)$ is unknown. So, instead of the first step proposed in Eq.(5.1), we choose appropriate values of K and σ. Thus we determine $V_c(r)$ as follows. Choosing the values of the scale parameter $\Lambda_{\rm QCD}$ and the off-diagonal gluon mass M, Eq.(3.4) determines the cut-off Λ_c. Then, substituting the values of Λ_c, K and σ into Eqs.(5.3)-(5.5), the quantities Q, m and r_c are determined numerically. As an example, we choose the values

$$\Lambda_{\rm QCD} = 0.2 \text{ GeV}, \quad M = 1.2 \text{ GeV}, \quad K = 0.3, \quad \sigma = 0.18 \text{ GeV}^2. \tag{5.6}$$

We note that the off-diagonal gluon mass $M \simeq 1.2$ GeV in the region of $r \gtrsim 0.2$ fm was obtained by using SU(2) lattice QCD in the maximal Abelian gauge [16]. The values $K \lesssim 0.3$ and $\sigma \lesssim 0.2$ GeV^2 come from lattice simulations [1].

[3] To determine the three parameters, it is natural to choose appropriate three points r_k $(k = 1, 2, 3)$. However, in the next step, we must determine V_c so as to the difference between V_c and V_{CL} becomes minimum. Since V_3 in V_c contains r in the integrand, it is difficult to determine r_k.

Now using the values of $\Lambda_{\rm QCD}$ and M in Eq.(5.6), Eq.(3.4) gives $\Lambda_c \simeq 2.03$ GeV. Next, we substitute this Λ_c and $(K,\ \sigma)$ in Eq.(5.6) into Eqs.(5.3)-(5.5), and solve these equations. The details are explained in Appendix B. The results are

$$r_c \simeq 1.145\ \text{GeV}^{-1} = 0.226\ \text{fm}, \quad a = m^2/\Lambda_c^2 \simeq 0.263,$$

and these values lead to

$$m = 1.04\ \text{GeV}, \quad K_c = \frac{Q^2}{4\pi} = 0.285, \quad \sigma_c = \frac{Q^2 m^2}{8\pi} \ln\left(\frac{\Lambda_c^2 + m^2}{m^2}\right) = 0.242\ \text{GeV}^2. \tag{5.7}$$

Thus we obtain

$$V_c(r) = \sum_{k=1}^{3} V_k(r), \quad V_1(r) = -\frac{0.285}{r}, \quad V_2(r) = 0.242 \cdot r, \quad V_3(r) = 0.747 \cdot S(r, 0.263), \tag{5.8}$$

where

$$S(r,a) = \int_0^{\Lambda_c r} dx \frac{\sin x}{x} \frac{ar}{x^2 + a(\Lambda_c r)^2}. \tag{5.9}$$

In Fig.3, the potentials $V_k(r), (k = 1, 2, 3)$ and $V_c(r)$ are plotted. Since $V_1(r) + V_3(r)$ is a substitute for the Yukawa potential, $V_1(r) + V_3(r) \approx 0$ for $r \gtrsim 0.35$ fm is reasonable. Using the values of $(K,\ \sigma)$ in Eq.(5.6), $V_{CL}(r)$ becomes

$$V_{CL}(r) = -\frac{0.3}{r} + 0.18 \cdot r. \tag{5.10}$$

Eqs.(5.8) and (5.10) are plotted in Fig. 4. Since $V_c(r)$ is fitted to $V_{CL}(r)$ at $r_c \simeq 0.226$ fm, they fit very well for 0.1 fm $\lesssim r \lesssim 0.4$ fm. However, when r becomes large, as $V_1(r) + V_3(r) \approx 0$ and $\sigma_c > \sigma$, $V_c(r) > V_{CL}(r)$ holds for $r \gtrsim 0.4$ fm. In the same way, $K_c < K$ leads to $V_c(r) > V_{CL}(r)$ for $r < 0.09$ fm.

6 The scales R_0 and $\tilde{R}_0$

In Sect. 5, the scale $r_c \simeq 0.226$ fm appears. On the other hand, considering the force $-V'(r)$, the intermediate scale R_0, which satisfies

$$r^2 V'(r)|_{r=R_0} = 1.65, \quad R_0 \simeq 0.5\ \text{fm}, \tag{6.1}$$

was proposed [11]. In successful potential models, this relation holds fairly well. For example, the $V_{CL}(r)$ with $(K = 0.52,\ \sigma = 0.183\ \text{GeV}^2)$ [3] gives $R_0 = 0.49$ fm. If we substitute $V_c(r)$

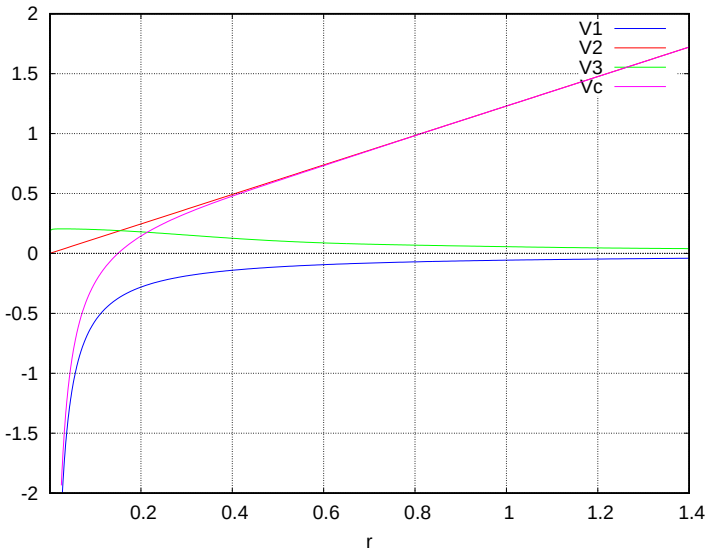


Fig. 3 The potentials V_1, V_2, V_3 and $V_c = \sum_{k=1}^{3} V_k$ in Eq.(5.8). The unit of r is fm, and the unit of the potentials is GeV.

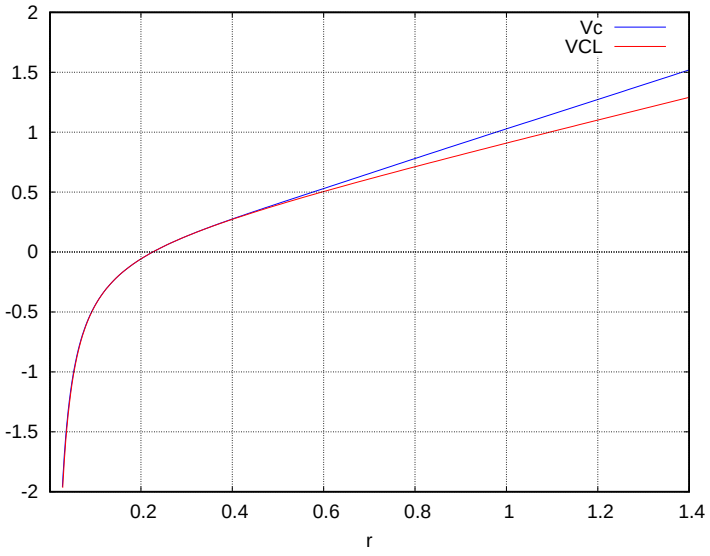


Fig. 4 The potentials V_c in Eq.(5.8) and V_{CL} with $(K = 0.3, \sigma = 0.18\ \mathrm{GeV}^2)$. Additive Constants are chosen to become $V_c(r_c) = V_{CL}(r_c) = 0$, and the unit of r is fm.

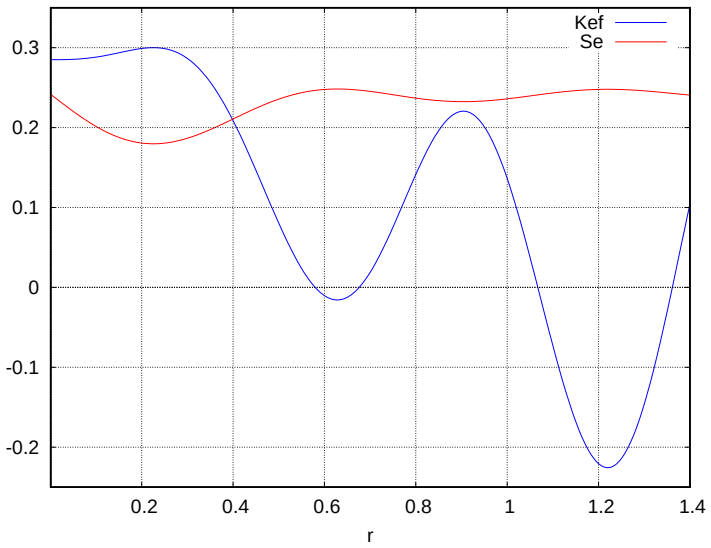


Fig. 5 The effective Coulomb coupling $K_{ef}(r) = K_c - \frac{r^3}{2}V_3''(r)$ and the effective string tension $S_e(r) = \sigma_{ef}(r) = \sigma_c + \frac{1}{2r}\left(r^2 V_3'(r)\right)'$. The unit of r is fm.

in Eq.(5.8) into Eq.(6.1), we obtain

$$K_{ef}(R_0) + R_0^2\sigma_{ef}(R_0) = 0.285 + 0.242R_0^2 + 0.747R_0^2 \cdot H(R_0, 0.263) = 1.65, \tag{6.2}$$

where

$$H(r,a) = \int_0^{\Lambda_c r} dx \left(\cos x - \frac{\sin x}{x}\right) \frac{a}{x^2 + a(\Lambda_c r)^2} \tag{6.3}$$

comes from $V_3'(r)$. Eq.(6.2) gives the solution $R_0 = 0.51$ fm. We note, $V_{CL}(r)$ with ($K = 0.3,\ \sigma = 0.18$ GeV^2) in Sect. 5 gives the larger value $R_0 = 0.54$ fm.

To see the meanings of these scales, the effective Coulomb coupling $K_{ef}(r) = K_c - \frac{r^3}{2}V_3''(r)$ in Eq.(5.3) and the effective string tension $\sigma_{ef}(r) = \sigma_c + \frac{1}{2r}\left(r^2 V_3'(r)\right)'$ in Eq.(5.4) are plotted in Fig. 5. We find $K_{ef}(r_c) = 0.3$ is the maximal value and $\sigma_{ef}(r_c) = 0.18$ GeV^2 is the minimal value. Namely r_c is the position where $K_{ef}(r)$ is maximum and $\sigma_{ef}(r)$ is minimum. We also notice that $K_{ef}(r) \approx 0$ at $r \approx 0.58$ fm, and 0.23 GeV$^2 < \sigma_{ef}(r) < 0.25$ GeV^2 for $r \gtrsim 0.5$ fm.

In Fig. 6, $r^2V_c'(r) = K_{ef}(r) + r^2\sigma_{ef}(r)$ and $r^2\sigma_{ef}(r)$ are plotted. We find that $r^2V_c'(r)$ satisfies $r^2V_c'(r) \approx K_{ef}(r)$ for $r < 0.2$ fm, and $r^2V_c'(r) \approx r^2\sigma_{ef}(r)$ for $r \gtrsim 0.5$ fm. Namely, the force-related quantity $r^2V_c'(r)$ is almost saturated with the string part $r^2\sigma_{ef}(r)$ above

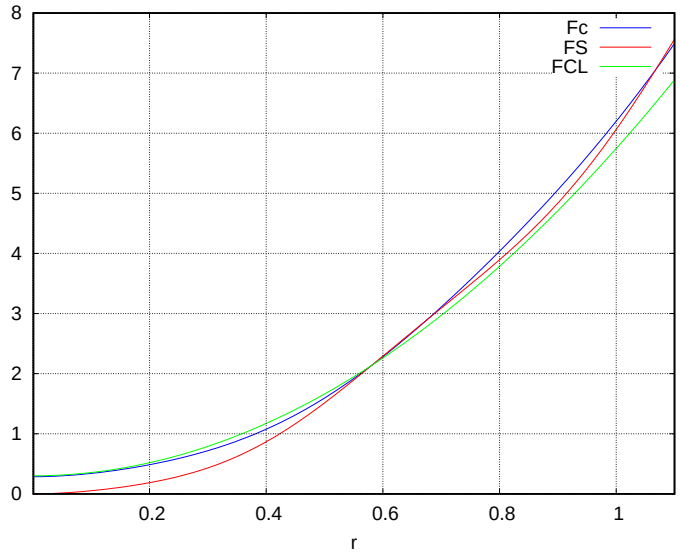


Fig. 6 $F_c(r) = r^2 V_c'(r) = K_{ef}(r) + r^2\sigma_{ef}(r)$ and $FS(r) = r^2\sigma_{ef}(r)$. For comparison, $FCL(r) = r^2 V_{CL}'(r) = K + r^2\sigma$ with $(K = 0.3, \sigma = 0.212\ \mathrm{GeV}^2)$ is plotted. The unit of r is fm.

$R_0 \simeq 0.5$ fm. Especially, as $K_{ef}(r) \approx 0$ at $r \approx 0.58$ fm, we find

$$r^2 V_c'(r)|_{r=\tilde{R}_0} \simeq r^2\sigma_{ef}(r)|_{r=\tilde{R}_0} = 2.13, \quad \tilde{R}_0 \simeq 0.58 \text{ fm}.$$

Before closing this section, based on the above analysis, we present the potential $V_{CL}(r)$ that fits to $V_c(r)$ better in the region of $r > 0.6$ fm. When r is small, the Coulomb part $K_{ef}(r)$ dominates. So keeping the condition Eq.(5.3) intact, we set $K = 0.3$. When r becomes large, the string part dominates. To determine the value of σ, it is reasonable to set the condition

$$r^2 V'(r)|_{r=\tilde{R}_0} = 2.13, \quad \tilde{R}_0 \simeq 0.58 \text{ fm}. \tag{6.4}$$

We find V_{CL} with $(K = 0.3, \sigma = 2.12\ \mathrm{GeV}^2)$ satisfies Eq.(6.4). We note this V_{CL} satisfies Eq.(6.1) as well.

In Fig. 7, the potential $V_c(r)$ and

$$V_{CL}(r) = -\frac{0.3}{r} + 2.12 \cdot r \tag{6.5}$$

are plotted . As we explained in Sect. 5, the behavior $V_c(r) > V_{CL}(r)$ comes about for large r. However Eq.(6.5) fits fairly well for $r < 1.2$ fm.

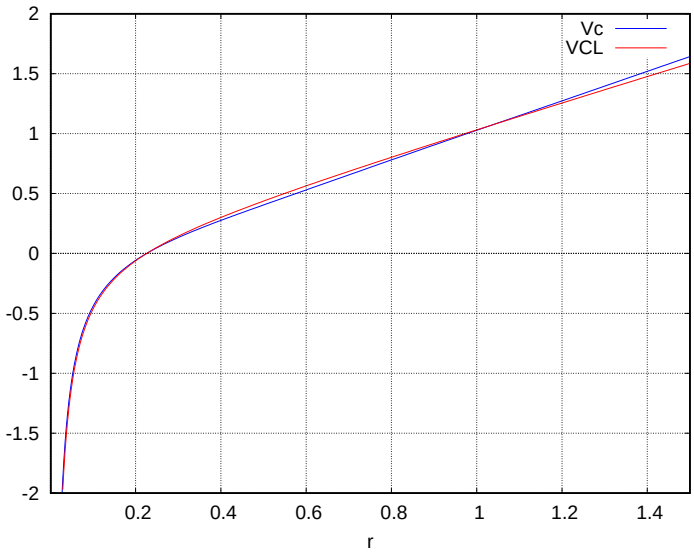


Fig. 7 The potentials V_c in Eq.(5.8) and V_{CL} with $(K = 0.3, \sigma = 0.212\ \text{GeV}^2)$. The unit of r is fm.

7 Summary and comments

In this paper, we considered the SU(2) gauge theory, and studied the $Q\bar{Q}$ potential Eq.(2.15). This potential is derived under the gauge field condensation. In Refs. [5–8], the dual Ginzburg-Landau model, which describes the monopole condensation, leads to the potential.

In our approach [9, 10], the ghost condensation $v \neq 0$ appears, and it induces the VEV $G^{(0)}_{\mu\mu}(x,x)$, that is the lowest term of $\langle A^+_\mu A^-_\mu \rangle$. If we divide the diagonal gluon as $A^3_\mu = a^3_\mu + b_\mu$, the classical part b_μ acquires the mass $m = g\sqrt{2G^{(0)}_{\mu\mu}(x,x)} \simeq g\Lambda_{\rm QCD}/\sqrt{32\pi}$, whereas the quantum part a^3_μ is massless. The off-diagonal gluons $A^\pm_\mu$ acquire the mass M through Eq.(3.3). The low energy effective Lagrangian is Eq.(2.9). As the classical solution b_μ, we choose the electric monopole solution of the dual gauge field $\mathcal{B}_\mu$ [10]. Then the propagator of $\mathcal{B}_\mu$ leads to the $Q\bar{Q}$ potential Eq.(2.15).

In calculating Eqs.(3.3) and (4.3), ultraviolet cut-off is necessary. Above the scale $\Lambda_{\rm QCD}$, although v vanishes, the masses M and m can exist. We assumed that these masses disappear above the cut-off Λ_c. Then the condition in Eq.(3.4) and the confining potential $V_c(r)$ in Eq.(4.10) are obtained. This potential has the linear potential $V_2(r)$ and, instead of the Yukawa potential, the Coulomb potential $V_1(r)$ and the additional term $V_3(r)$.

Although we derived $V_c(r)$, there are unknown parameters. To determine them, we chose the values presented in Eq.(5.6). Then, from Eq.(3.4), the cut-off $\Lambda_c = 2.03$ GeV was obtained. Next, assuming that the Cornell potential $V_{CL}(r)$ with $(K = 0.3, \sigma = 0.18 \text{ GeV}^2)$ describes a true potential well at some point r_c, we required $V_c(r) \simeq V_{CL}(r)$ near $r = r_c$. To realize this requirement, the conditions in Eq.(5.2) are imposed. By solving these conditions, $r_c \simeq 0.226$ fm, the values of m and Q^2 in Eq.(5.7), and $V_c(r)$ in Eq.(5.8) were obtained.

There are two implicit scales r_c and R_0 (or $\tilde{R}_0$) in $V_c(r)$. To understand them, the effective Coulomb coupling $K_{ef}(r)$ in Eq.(5.3) and the effective string tension $\sigma_{ef}(r)$ in Eq.(5.4) were studied. Since $V_3(r)$ contributes to them, they depend on r. At $r = r_c$, $K_{ef}(r)$ becomes maximum and $\sigma_{ef}(r)$ becomes minimum. For $r > R_0 \simeq 0.5$ fm, $0.23 \text{ GeV}^2 < \sigma_{ef}(r) < 0.25 \text{ GeV}^2$ holds.

If we consider the quantity $r^2 V_c'(r) = K_{ef}(r) + r^2 \sigma_{ef}(r)$, we find

$$r^2 V_c'(r) \approx \begin{cases} K_{ef}(r), & (r < 0.2 \text{ fm}) \\ r^2 \sigma_{ef}(r), & (r > 0.5 \text{ fm}). \end{cases}$$

Namely the main force between Q and $\bar{Q}$ is the effective Coulomb force $-K_{ef}/r^2$ for $r < r_0$, and the effective string force $-\sigma_{ef}(r)$ for $r > R_0$.

Although $V_c(r)$ was determined to fit to $V_{CL}(r)$ with $(K = 0.3, \sigma = 0.18 \text{ GeV}^2)$ at $r = r_c$, it becomes larger than $V_{CL}(r)$ for $r > 0.4$ fm. The Cornell potential is often used to fit lattice simulation data. Can we find $V_{CL}(r)$ that fits to $V_c(r)$ better? To answer this question, we used the above scales. At r_c, Eq.(5.3) was applied to determine K. To determine σ, we used Eq.(6.4) at $\tilde{R}_0$. Then we obtained $V_{CL}(r)$ with $(K = 0.3, \sigma = 0.212 \text{ GeV}^2)$. This potential satisfies Eq.(6.1) at R_0 as well, and fits fairly well in the region of $r < 1.2$ fm.

We make three comments.

(1). In quark confinement, Abelian dominance [17] is expected. The lattice simulation in the maximal Abelian gauge shows that the linear part of the $Q\bar{Q}$ potential comes from the Abelian part [18]. In the present case, Abelian dominance is realized by the massive classical U(1) field $\mathcal{B}_\mu$. This field brings about the potential $V_c(r)$.

(2) Although $V_c(r)$ comes from $\mathcal{B}_\mu$, to determine its behavior, information on the fields a_μ^A for $\Lambda_{\rm QCD} < \mu < \Lambda_c$ is necessary. The low energy Lagrangian (2.9) will be modified in this region. However, as the first approximation, we used Eq. (2.9) and assumed the cut-off Λ_c for m.

(3). The values of r_c, $\tilde{R}_0$, m and Q^2 in Eq.(5.7) depend on the choice of Eq.(5.6). However the existence of these scales, and the behavior of $V_c(r)$, e.g., $\lim_{r\to\infty} V_3(r) = 0$, $\sigma_c > \sigma$, $K_c < K$, and $V_c(r) > V_{CL}(r)$ for large r, are unchanged.

A Propagator $G^{(0)}_{\mu\nu}(y,x)$ for A^a_μ

Referring to Eqs.(2.2) and (2.9), we consider the Lagrangian with the massive gauge fields $A^\pm_\mu = (A^1_\mu \pm iA^2_\mu)/\sqrt{2}$:

$$\sum_{a=1}^{2}\left\{\frac{1}{4}(\partial\wedge A^a)^2_{\mu\nu}+\frac{M^2}{2}(A^a_\mu)^2-\frac{\alpha_1}{2}(B^a)^2+B^a(\partial_\mu A^a_\mu+\varphi^a)+\frac{(\varphi^a)^2}{2\alpha_2}\right\}.$$

The fields A_μ, B and φ mix. The inverse propagators of these fields are

$$\begin{array}{c} \\ A_\mu \\ B \\ \varphi \end{array}\begin{array}{c} \begin{array}{ccc} A_\nu & B & \varphi \end{array} \\ \begin{pmatrix} (p^2+M^2)P^T_{\mu\nu}+M^2P^L_{\mu\nu} & -ip_\mu & 0 \\ ip_\nu & -\alpha_1 & 1 \\ 0 & 1 & \frac{1}{\alpha_2} \end{pmatrix} \end{array}, \tag{A1}$$

and the corresponding propagators are

$$\begin{array}{c} \\ A_\mu \\ B \\ \varphi \end{array}\begin{array}{c} \begin{array}{ccc} A_\nu & B & \varphi \end{array} \\ \begin{pmatrix} \frac{1}{p^2+M^2}P^T_{\mu\nu}+\frac{(\alpha_1+\alpha_2)}{\Xi}P^L_{\mu\nu} & \frac{-ip_\mu}{\Xi} & \frac{ip_\mu\alpha_2}{\Xi} \\ \frac{ip_\nu}{\Xi} & \frac{-M^2}{\Xi} & \frac{\alpha_2M^2}{\Xi} \\ \frac{-ip_\nu\alpha_2}{\Xi} & \frac{\alpha_2M^2}{\Xi} & \frac{\alpha_2(p^2+\alpha_1M^2)}{\Xi} \end{pmatrix} \end{array}, \tag{A2}$$

where $\Xi = p^2+(\alpha_1+\alpha_2)M^2$, and

$$P^T_{\mu\nu}=\delta_{\mu\nu}-\frac{p_\mu p_\nu}{p^2},\quad P^L_{\mu\nu}=\frac{p_\mu p_\nu}{p^2}.$$

Under the BRS transformation δ_B, as $\delta_B\bar{c}=iB$ and $\delta_B B=0$,

$$\langle BB\rangle = -i\langle\delta_B(\bar{c}B)\rangle = 0$$

holds, if the BRS symmetry is not broken spontaneously. When $M\neq 0$, to make

$$\langle BB\rangle = \frac{-M^2}{p^2+(\alpha_1+\alpha_2)M^2}$$

vanish, we choose $\alpha_2\to\infty$. Then Eq.(A2) becomes

$$\begin{array}{c} \\ A_\mu \\ B \\ \varphi \end{array}\begin{array}{c} \begin{array}{ccc} A_\nu & B & \varphi \end{array} \\ \begin{pmatrix} \frac{1}{p^2+M^2}P^T_{\mu\nu}+\frac{1}{M^2}P^L_{\mu\nu} & 0 & \frac{ip_\mu}{M^2} \\ 0 & 0 & 1 \\ \frac{-ip_\nu}{M^2} & 1 & \frac{p^2+\alpha_1M^2)}{M^2} \end{pmatrix} \end{array}.. \tag{A3}$$

Eq.(A3) shows that A_μ mixes with φ. At the one-loop order, the ghost loop contributes to $\langle A_\mu A_\nu\rangle$, $\langle A_\mu\varphi\rangle$ and $\langle\varphi\varphi\rangle$ as well. However tachyonic behavior only appears in $\langle A_\mu A_\nu\rangle$. In

Sect. 3, as the mixing like $\langle A_\mu \varphi \rangle$ does not contribute, the propagator

$$G^{(0)}_{\mu\nu}(p) = \frac{1}{p^2 + M^2} P^T_{\mu\nu} + \frac{1}{M^2} P^L_{\mu\nu}$$

in Eq.(A3) is used.

B Solution of Eqs.(5.3)-(5.5)

From Eq.(4.9), we find the derivatives

$$\begin{aligned}
V_3'(r) &= Q^2 \frac{m^2}{2\pi^2} \int_0^{\Lambda_c} dq \left(\frac{\cos qr}{r} - \frac{\sin qr}{qr^2} \right) \frac{1}{q^2 + m^2}, \\
V_3''(r) &= Q^2 \frac{m^2}{2\pi^2} \int_0^{\Lambda_c} dq \left(2\frac{\sin qr}{qr^3} - 2\frac{\cos qr}{r^2} - \frac{q \sin qr}{r} \right) \frac{1}{q^2 + m^2}, \\
\left(r^3 V_3''(r) \right)' &= Q^2 \frac{m^2}{2\pi^2} \int_0^{\Lambda_c} dq \left(-q^2 r^2 \cos qr \right) \frac{1}{q^2 + m^2}.
\end{aligned}$$

Then, introducing the variables $x = qr$ and $a = m^2/\Lambda_c^2$, Eqs.(5.3)-(5.5) become

$$K = \frac{Q^2}{4\pi} \left[1 + \frac{\Lambda_c^2}{\pi} r_c^2 \left\{ 2H(r_c, a) + L(r_c, a) \right\} \right], \tag{B1}$$

$$\sigma = \frac{Q^2}{4\pi} \left\{ \frac{\Lambda_c^2}{2} a \ln \left(1 + \frac{1}{a} \right) - \frac{\Lambda_c^2}{\pi} L(r_c, a) \right\}, \tag{B2}$$

$$G(r_c, a) = \int_0^{\Lambda_c r_c} dx \frac{x^2 \cos x}{x^2 + a(\Lambda_c r_c)^2} = 0, \tag{B3}$$

where $H(r, a)$ is defined in Eq.(6.3), and

$$L(r, a) = \int_0^{\Lambda_c r} dx x \sin x \frac{a}{x^2 + a(\Lambda_c r)^2}.$$

By eliminating Q^2, Eqs.(B1) and (B2) leads to

$$F(r_c, a) = \sigma + 2\sigma \frac{\Lambda_c^2}{\pi} r_c^2 H(r_c, a) + \frac{\Lambda_c^2}{\pi} \left(\sigma r_c^2 + K \right) L(r_c, a) - K \frac{\Lambda_c^2}{2} a \ln \left(1 + \frac{1}{a} \right) = 0. \tag{B4}$$

Now we substitute $K = 0.3, \sigma = 0.18$ GeV^2 and $\Lambda_c = 2.03$ GeV. To solve Eq.(B3) and Eq.(B4) numerically, choosing $a = 0.2, 0.263$ and 0.3, $G(r, a)$ and $F(r, a)$ are plotted in Fig. B1 and Fig. B2, respectively. We find that $G(r_c, a) = 0$ and $F(r_c, a) = 0$ give the solutions $a \simeq 0.263$ and $r_c \simeq 1.145 \text{GeV}^{-1}$.

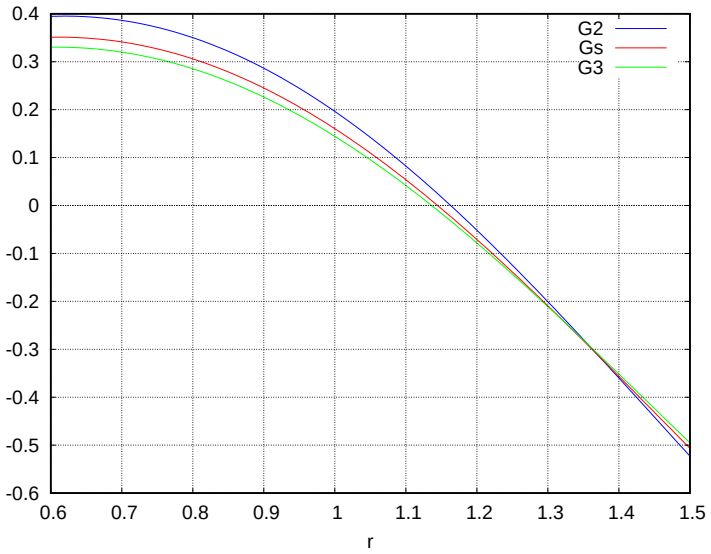


Fig. B1 The behavior of the function $G(r,a)$. $G2 = G(r, 0.2)$, $G3 = G(r, 0.3)$ and $Gs = G(r, 0.263)$ are plotted. The unit of r is GeV^{-1}. $Gs = 0$ holds at $r \simeq 1.145\ \mathrm{GeV}^{-1}$.

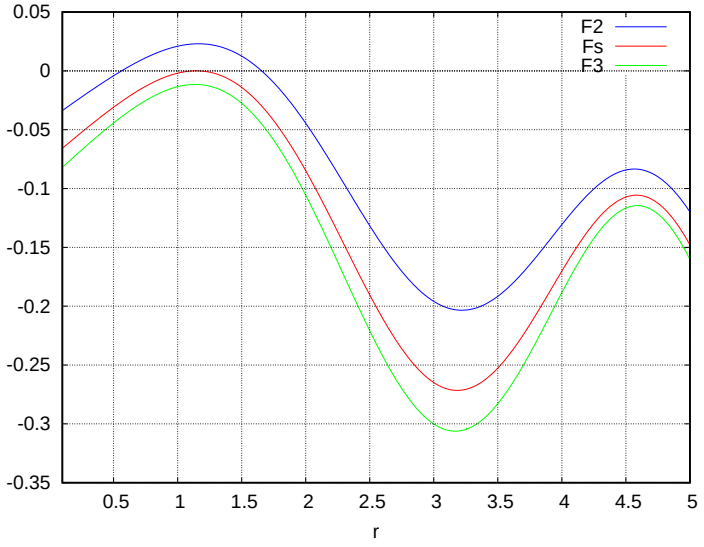


Fig. B2 The behavior of the function $F(r,a)$. $F2 = F(r, 0.2)$, $F3 = F(r, 0.3)$ and $Fs = F(r, 0.263)$ are plotted. The unit of r is GeV^{-1}. $Fs = 0$ holds at $r \simeq 1.145\ \mathrm{GeV}^{-1}$.

Using these values, Eqs.(B1) and (B2) give

$$K_c = \frac{Q^2}{4\pi} \simeq 0.285, \quad \sigma_c = \frac{Q^2}{4\pi}\frac{\Lambda_c^2}{2} a \ln\left(1+\frac{1}{a}\right) \simeq 0.242 \text{ GeV}^2.$$

In the same way, using $S(r,a)$ in Eq.(5.9), Eq.(4.9) becomes

$$V_3(r) = 2\frac{Q^2}{4\pi}\frac{\Lambda_c^2}{\pi} S(r, 0.263) = 0.747 \cdot S(r, 0.263). \tag{B5}$$

References

[1] G. Bali, Phys. Rept. **343**, 1 (2001).
[2] E. Eichten et al., Phys. Rev. Lett. **34**, 369 (1975).
[3] E. Eichten et al., Phys. Rev. D **21**, 203 (1980).
[4] G. Ripka, arXiv:hep-ph/0310102.
[5] T. Suzuki, Prog. Theor. Phys. **80**, 929 (1988).
[6] S. Maedan and T. Suzuki, Prog. Theor. Phys. **81**, 229 (1989).
[7] S. Sasaki, H. Suganuma and H. Toki, Prog. Theor. Phys. **94**, 373 (1995).
[8] H. Suganuma, S. Sasaki and H. Toki, Nucl. Phys. B **435**, 207 (1995).
[9] H. Sawayanagi, Prog. Theor. Exp. Phys. **2019**, 033B03 (2019).
[10] H. Sawayanagi, Prog. Theor. Exp. Phys. **2017**, 113B02 (2017).
[11] R. Sommer, Nucl. Phys. B **411**, 839 (1994).
[12] G. Curci and R. Ferrari, Phys. Lett. **B63**, 91 (1976).
[13] H. Sawayanagi, Phys. Rev. D **67**, 045002 (2003).
[14] H. Sawayanagi, Prog. Theor. Phys. **117**, 305 (2007).
[15] D. Zwanziger, Phys. Rev. D **3**, 880 (1971).
[16] K. Amemiya and H. Suganuma, Phys. Rev. D **60**, 114509 (1999).
[17] Z. F. Ezawa and A. Iwazaki, Phys. Rev. D **25**, 2681 (1982).
[18] N. Sakumichi and H. Suganuma, Phys. Rev. D **90**, 111501(R) (2014).